RPA Interacts with HIRA and Regulates H3.3 Deposition at Gene Regulatory Elements in Mammalian Cells

Honglian Zhang[1, 5], Haiyun Gan[1, 5], Zhiquan Wang[2, 5], Jeong-Heon Lee[2], Hui Zhou[1], Tamas Ordog[2], Marc S. Wold[3], Mats Ljungman[4] and Zhiguo Zhang[1, 2, *]

[1]Department of Pediatrics
Department of Genetics and Development
Institute for Cancer Genetics
College of Surgeons and Physicians
Columbia University
1130 St. Nicholas Avenue
Irving Cancer Research Center
New York, NY10032

[2]Center for Individualized Medicine
Mayo Clinic College of Medicine, Rochester, MN, 55905, USA

[3]Department of Biochemistry, Carver College of Medicine,
University of Iowa, Iowa City, IA, 52242, USA

[4]Departments of Radiation Oncology and Environmental
Health Sciences Translational Oncology Program and Center for RNA Biomedicine,
University of Michigan Medical School, Ann Arbor, MI, 48109, USA

[5] These authors contributed equally to this work

[*]Corresponding author: zz2401@cumc.columbia.edu

(p): 212-851-4936

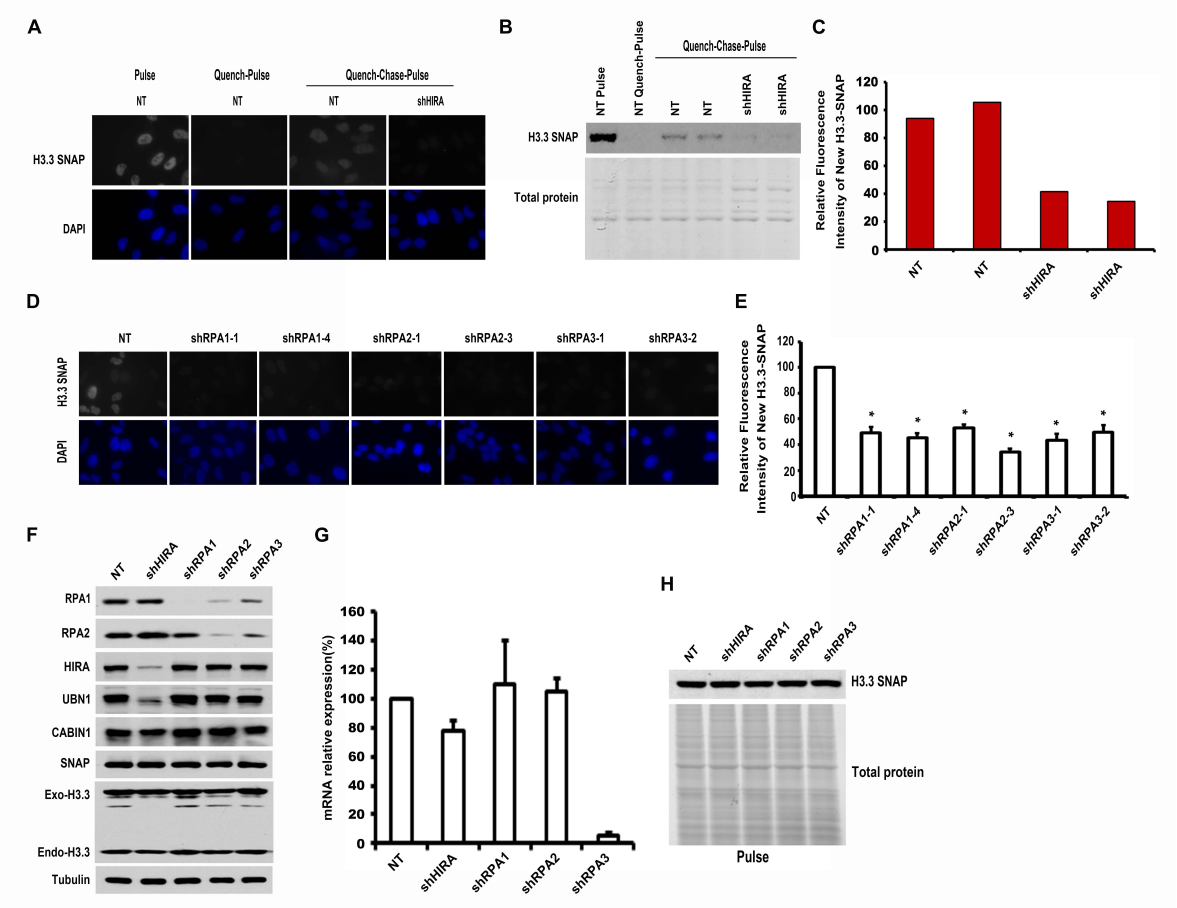
A
Pulse
Quench-Pulse
Quench-Chase-Pulse
NT
NT
NT
shHIRA
H3.3 SNAP
DAPI
B
NT Pulse
NT Quench-Pulse
Quench-Chase-Pulse
NT
NT
shHIRA
shHIRA
H3.3 SNAP
Total protein
C
Relative Fluorescence Intensity of New H3.3-SNAP
120
100
80
60
40
20
0
NT
NT
shHIRA
shHIRA
D
NT
shRPA1-1
shRPA1-4
shRPA2-1
shRPA2-3
shRPA3-1
shRPA3-2
H3.3 SNAP
DAPI
E
Relative Fluorescence Intensity of New H3.3-SNAP
120
100
80
60
40
20
0
*
NT
shRPA1-1
shRPA1-4
shRPA2-1
shRPA2-3
shRPA3-1
shRPA3-2
F
NT
shHIRA
shRPA1
shRPA2
shRPA3
RPA1
RPA2
HIRA
UBN1
CABIN1
SNAP
Exo-H3.3
Endo-H3.3
Tubulin
G
mRNA relative expression(%)
160
140
120
100
80
60
40
20
0
NT
shHIRA
shRPA1
shRPA2
shRPA3
H
NT
shHIRA
shRPA1
shRPA2
shRPA3
H3.3 SNAP
Total protein
Pulse

Figure S1. Validation of the SNAP Staining Assay for Monitoring the Deposition of Newly Synthesized H3.3.

(A-C) Depletion of HIRA results in reduced deposition of newly synthesized H3.3 based on analysis of fluorescence intensity at individual cells using fluorescence microscopy (A) or using a chromatin fractionation assay (B-C). As a proof of concept, HIRA depleted cells were used as control. HeLa cells stably expressing H3.3-SNAP were infected with viruses expressing non-targeting (NT) or shHIRA. 72 h after infection, cells were treated differently: "pulse" labels pre-existing H3.3-SNAP without blocking and chasing; the "quench-pulse" quenches pre-existing H3-SNAP without chasing, and "quench-chase-pulse" involves in block pre-existing H3.3-SNAP and labeling new H3.3-SNAP synthesized during the 12 h chasing after removing blocking reagent. (A) Cells were fixed for immunofluorescence to detect H3.3-SNAP under three different treatments, and the typical image of fluorescence intensity using fluorescence microscopy was shown. (B) Cells were also used to perform chromatin fractionation assays, and proteins in chromatin fractions were resolved using a SDS-PAGE. (C) The fluorescence intensity of H3.3-SNAP was detected using a Typhoon FLA 7000, and total proteins were visualized by IRDye Blue Protein Stain. Image J was used to quantify the SNAP fluorescence intensity and total protein levels. The relative SNAP intensity was the ratio of H3.3-SNAP fluorescence intensity over total protein levels and the relative intensity in NT cells was set to 100. (D-E) Depletion of each subunit of the RPA complex affects the deposition of newly synthesized H3.3 as detected by H3.3-SNAP intensity in individual cells using fluorescence microscopy. HeLa cells stably expressing H3.3-SNAP were infected with viruses expressing two individual shRNAs targeting each RPA subunit. (D) The deposition of newly synthesized

H3.3 was analyzed by fluorescence microscope. (E) The relative fluorescence intensity of H3.3-SNAP compared to in NT cells from three independent experiments was calculated and reported (mean±SD, * $p < 0.05$). For each sample, fluorescence intensity of at least 100 cells was counted. (F-H). Depletion of RPA does not affect the total levels of H3.3-SNAP and expression of HIRA, UBN1 and CABIN1. (F-G) Depletion of RPA does not affect expression of each subunit of HIRA complex. The expression levels of RPA1, RPA2, H3.3-SNAP and three subunits of HIRA complex were detected by Western blot in cells depleted with HIRA or each subunit of RPA complex. (G) The expression level of RPA3 was detected by real time RT-PCR in HIRA, RPA1, RPA2 or RPA3 depleted cells. Because antibodies against RPA3 were not available, we analyzed the effect of deletion of HIRA, RPA1, RPA2 and RPA3 on the expression of RPA3 by RT-PCR. The results represent the average of two independent experiments. (H) Depletion of HIRA or each subunit of the RPA complex does not affect total levels of H3.3-SNAP level. Total levels of H3.3-SNAP were detected by TMR without blocking and chasing (pulse). **Related to Figure 1.**

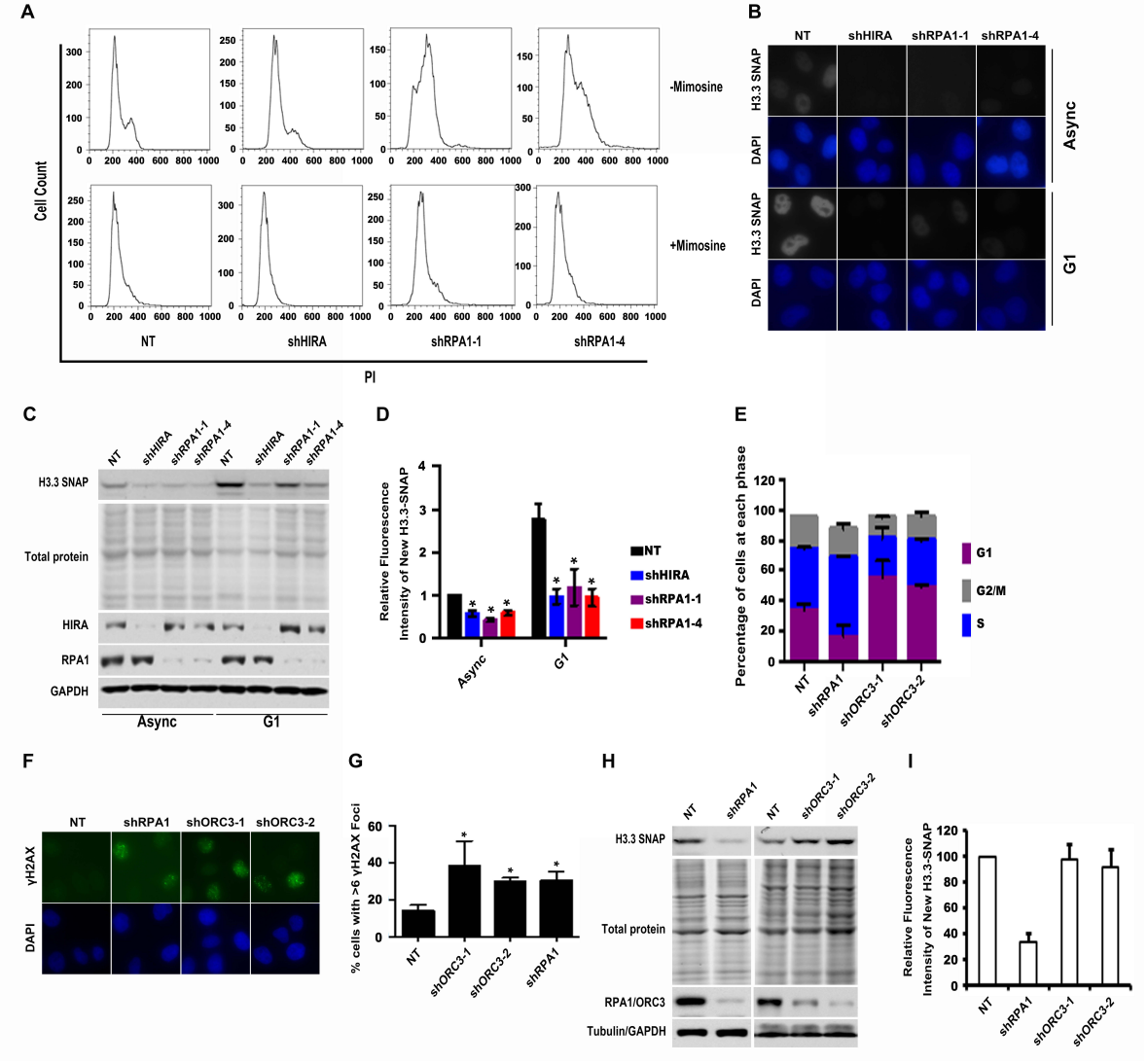
A
Cell Count
PI
-Mimosine
+Mimosine
NT
shHIRA
shRPA1-1
shRPA1-4
B
NT
shHIRA
shRPA1-1
shRPA1-4
H3.3 SNAP
DAPI
Async
G1
C
H3.3 SNAP
Total protein
HIRA
RPA1
GAPDH
Async
G1
D
Relative Fluorescence Intensity of New H3.3-SNAP
NT
shHIRA
shRPA1-1
shRPA1-4
Async
G1
E
Percentage of cells at each phase
G1
G2/M
S
NT
shRPA1
shORC3-1
shORC3-2
F
NT
shRPA1
shORC3-1
shORC3-2
γH2AX
DAPI
G
% cells with >6 γH2AX Foci
NT
shORC3-1
shORC3-2
shRPA1
H
H3.3 SNAP
Total protein
RPA1/ORC3
Tubulin/GAPDH
I
Relative Fluorescence Intensity of New H3.3-SNAP
NT
shRPA1
shORC3-1
shORC3-2

Figure S2. RPA Regulates H3.3 Deposition at G1 Phase of the Cell Cycle.

(A-D) Depletion of RPA and HIRA in G1 cells affects the deposition of newly synthesized H3.3. HeLa cells stably expressing H3.3-SNAP were infected with viruses expressing one shRNA targeting HIRA or two different shRNAs targeting RPA1. Sixty hours after infection, cells were treated with or without 0.2 mM mimosine for 16 hours to arrest cells at G1 phase. (A) Mimosine treatment results in G1 cell cycle arrest as determined by flow cytometry. The deposition of newly synthesized H3.3 was analyzed by fluorescence microscopy (B) as well as chromatin fractionation assays (C-D). H3.3-SNAP, total proteins as well as HIRA and RPA1 levels were analyzed as described in Figure 1. The relative SNAP intensity in NT cells, HIRA and RPA1 depleted cells was quantified and reported as the (mean±SEM) of three independent experiments (* $p < 0.05$). (E-I) Depletion of ORC3 does not affect H3.3 deposition. (E) Depletion of RPA1 or ORC3 leads to cell cycle defects. The cell cycle progression of RPA1, ORC3 depleted or control cells were monitored by Brdu/PI flow cytometry and percentage of cells at each phase of the cell cycle was quantified and shown in E (mean±SEM, N=3). (F-G) Depletion of RPA1 or ORC3 results in increased spontaneous DNA damage. (F) Immunofluorescence using antibodies against γ-H2AX in RPA1 or ORC3 depleted cells was performed. (G) Cells with more than 6 γ H2AX foci were counted and reported as the mean and SD from three independent experiments (mean ±SEM, N=3, $p< 0.01$). (H-I) Depletion of ORC3, in contrast to RPA depletion, does not affect H3.3 deposition. The H3.3 deposition was monitored by CFAs (H) the relative SNAP intensity from three independent experiments was shown in (I). **Related to Figure 1.**

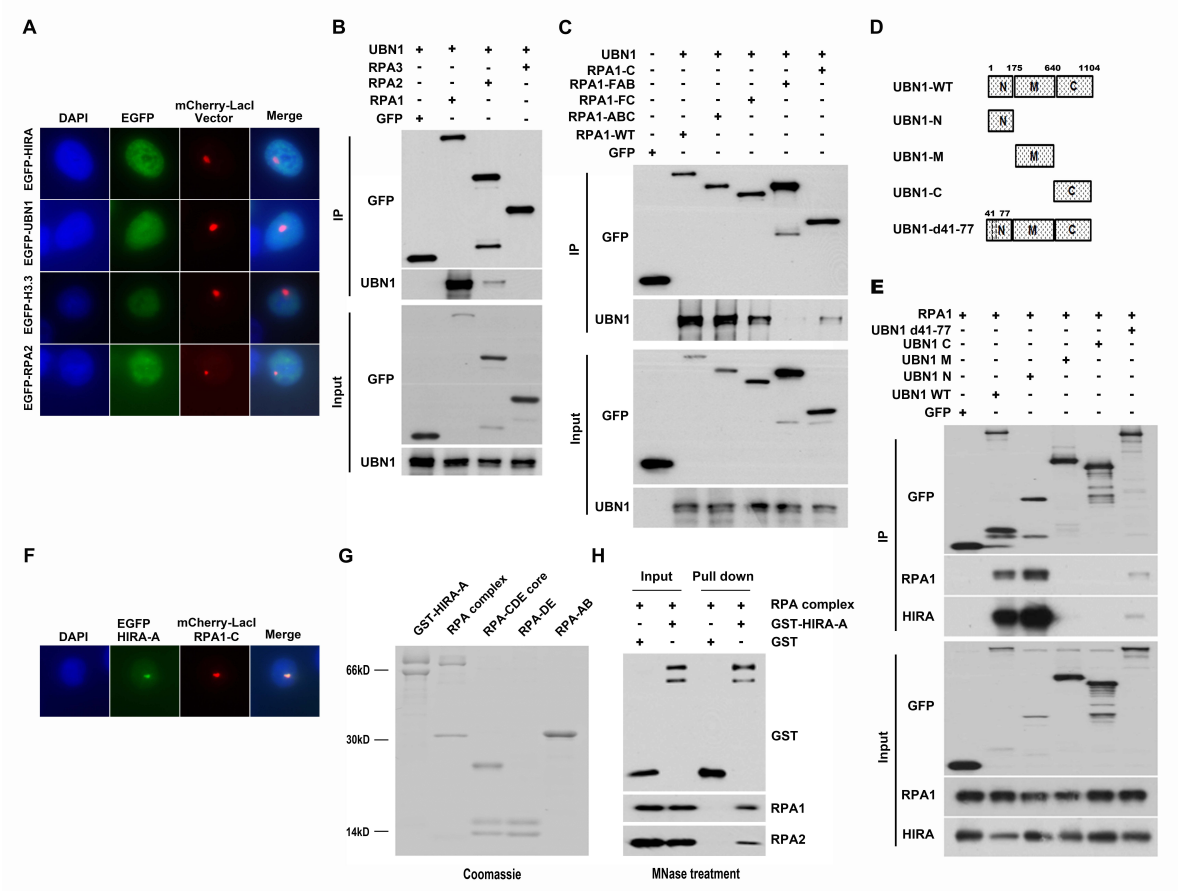
A
DAPI
EGFP
mCherry-LacI Vector
Merge
EGFP-HIRA
EGFP-UBN1
EGFP-H3.3
EGFP-RPA2
B
UBN1
RPA3
RPA2
RPA1
GFP
IP
GFP
UBN1
Input
GFP
UBN1
C
UBN1
RPA1-C
RPA1-FAB
RPA1-FC
RPA1-ABC
RPA1-WT
GFP
IP
GFP
UBN1
Input
GFP
UBN1
D
1
175
640
1104
UBN1-WT
N
M
C
UBN1-N
N
UBN1-M
M
UBN1-C
C
41 77
UBN1-d41-77
N
M
C
E
RPA1
UBN1 d41-77
UBN1 C
UBN1 M
UBN1 N
UBN1 WT
GFP
IP
GFP
RPA1
HIRA
Input
GFP
RPA1
HIRA
F
DAPI
EGFP HIRA-A
mCherry-LacI RPA1-C
Merge
G
GST-HIRA-A
RPA complex
RPA-CDE core
RPA-DE
RPA-AB
66kD
30kD
14kD
Coomassie
H
Input
Pull down
RPA complex
GST-HIRA-A
GST
GST
RPA1
RPA2
MNase treatment

Figure S3. The UBN1-RPA interaction is mediated through HIRA.

(A) HIRA-, UBN1-, H3.3- or RPA2-EGFP does not form foci with LacI empty vector. HIRA-, UBN1-, H3.3- or RPA2-EGFP was co-transfected into A03_1 cells with mCherry-LacI-empty vector, and cells were visualized using fluorescence microscopy. (B) RPA1 interacts with UBN1. RPA1-, RPA2- or RPA3-EGFP was co-transfected with UBN1-mCherry-LacI in 293T cells. Proteins were immunoprecipitated using antibodies against GFP and analyzed by Western blot. (C) RPA1-C domain interacts with UBN1. (D) Schematic representation of UBN1 deletion mutants. (E) UBN1-N domain interacts with RPA1 and mutations at the HIRA binding site (d41-77) compromise the interaction between UBN1 and RPA1. The experiments in C and E were performed as described in B. (F) RPA1-C domain interacts with HIRA-A domain. HIRA-A-EGFP was co-transfected into A03_1 cells with mCherry-LacI-RPA1-C, and cells were visualized using fluorescence microscopy. (G) Recombinant proteins used in vitro studies in Figure 3. GST-tagged HIRA-A domain, RPA complex, RPA-CDE core, RPA 2, 3-DE and RPA1-AB domain were purified from *E.coli*, separated on SDS-PAGE and visualized using Coomassie blue staining. (H) The RPA complex interacts with HIRA-A domain *in vitro*. GST or GST-HIRA-A proteins immobilized on GST beads were used to pull down recombinant RPA complex after MNase (Micrococcal nuclease) treatment. **Related to Figure 2 and 3.**

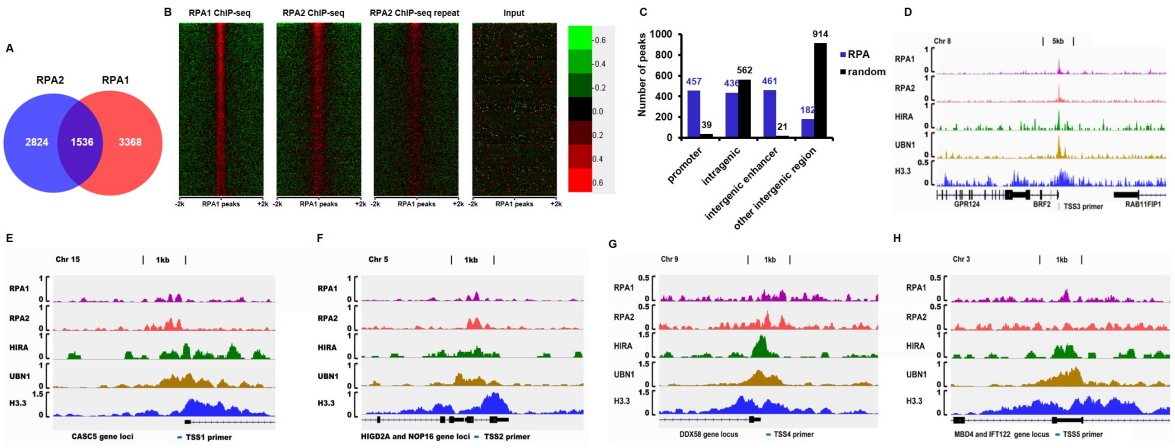

Figure S4. RPA1 and RPA2 Co-localize at Gene Regulatory Elements.

(A-B) RPA1 and RPA2 co-localize on chromatin. (A) Venn diagram illustration of RPA1 and RPA2 ChIP-seq peaks in HeLa cell. (B) RPA2 co-localizes with RPA1 on chromatin. The plot shows the reads density of RPA2 ChIP-seq surrounding RPA1 ChIP-seq peaks. A 40 bp window around PRA1 peaks was used to calculate RPA2 ChIP-seq reads density from two independent repeats and ranked by p value of enrichment. Input was used as a native control. (C) Genomic distribution of RPA1 and RPA2 ChIP-seq overlapping peaks. Random peak sets were chosen from the hg19 genome annotation with the same length as the RPA peaks. Promoters were defined as from 2 Kb upstream to 1 Kb downstream of TSS (Zhang, 2003); intragenic region is from TSS to TES, and the remaining region is defined as intergenic. HeLa enhancer datasets were obtained from published work (Hnisz et al., 2013) but only the intergenic enhancers were used to annotate RPA peaks. RPA peaks that overlap more than one feature were assigned only to one region in the order of promoter > intragenic > intergenic enhancer > other intergenic region. (D-H) RPA1 and

RPA2 co-localize with HIRA, UBN1 and H3.3 genome-wide. Integrative Genomics Viewer (IGV) tracks show the distribution of RPA1, RPA2, HIRA, UBN1, and H3.3 at multiple genes (D, longer track) *CASC5* (E), *HIGD2A* and *NOP16* gene loci (F), *DDX58* (G), *MBD4* and *IFT122* gene loci (H). **Related to Figure 4.**

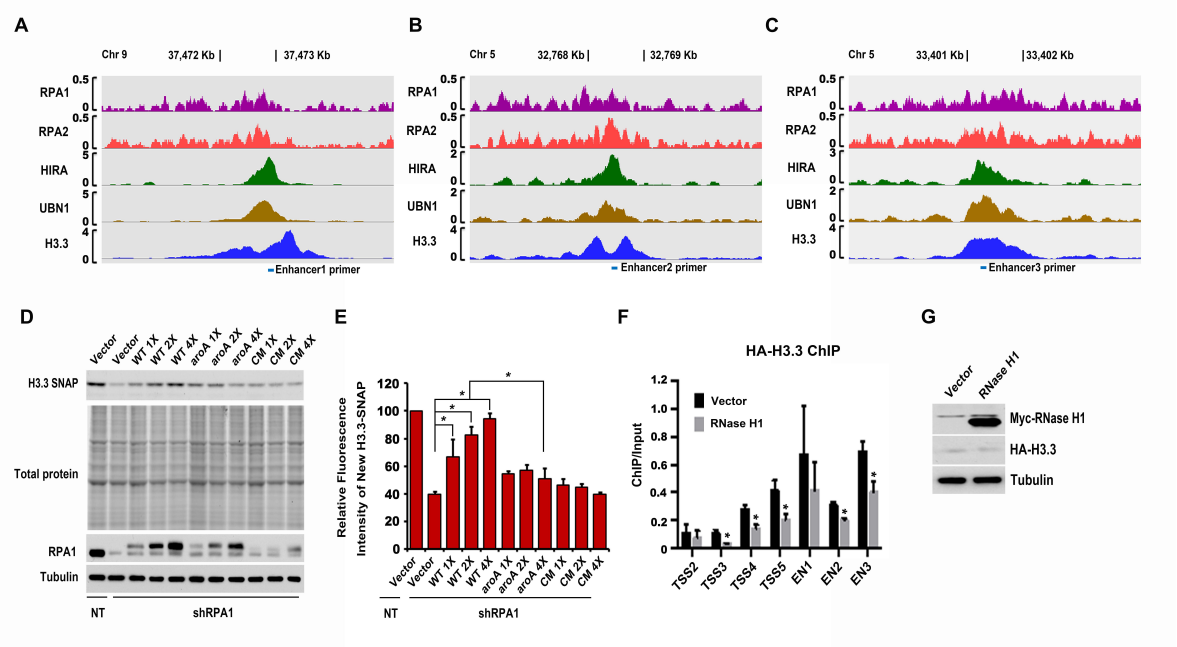
A
Chr 9
37,472 Kb |
| 37,473 Kb
RPA1
RPA2
HIRA
UBN1
H3.3
Enhancer1 primer
B
Chr 5
32,768 Kb |
| 32,769 Kb
RPA1
RPA2
HIRA
UBN1
H3.3
Enhancer2 primer
C
Chr 5
33,401 Kb |
|33,402 Kb
RPA1
RPA2
HIRA
UBN1
H3.3
Enhancer3 primer
D
Vector
Vector
WT 1X
WT 2X
WT 4X
aroA 1X
aroA 2X
aroA 4X
CM 1X
CM 2X
CM 4X
H3.3 SNAP
Total protein
RPA1
Tubulin
NT
shRPA1
E
Relative Fluorescence Intensity of New H3.3-SNAP
120
100
80
60
40
20
0
Vector
Vector
WT 1X
WT 2X
WT 4X
aroA 1X
aroA 2X
aroA 4X
CM 1X
CM 2X
CM 4X
NT
shRPA1
F
HA-H3.3 ChIP
ChIP/Input
1.2
1.0
0.8
0.6
0.4
0.2
0
Vector
RNase H1
TSS2
TSS3
TSS4
TSS5
EN1
EN2
EN3
G
Vector
RNase H1
Myc-RNase H1
HA-H3.3
Tubulin

Figure S5. The Ability of RPA1 to Bind to ssDNA Is Required for H3.3 Deposition.

(A-C) Representative ChIP-seq tracks for the enhancer regions that are used for experiments shown in Figure 5. IGV tracks show the distribution of RPA1, RPA2, HIRA, UBN1 and H3.3 at three chosen enhancers. (D-E) The RPA1-aroA mutant is defective to rescue the H3.3 deposition defects in RPA1 depleted cells compared to wild type RPA1. (D) HeLa cells stably expressing H3.3-SNAP were infected with three different amounts of lenti-virus expressing shRNA-resistant WT RPA1 and two RPA1 mutants (CM and aroA). The deposition of newly synthesized H3.3 was monitored by chromatin fractionation assays as described in Figure 1. (E) The relative SNAP intensity in NT cells and RPA1 depleted cells expressing WT RPA1 or RPA1 mutant was calculated and reported as the average and standard deviation of three independent experiments (mean ±SD, * $p < 0.05$). Since the expression of wild type RPA1 at 2X virus was similar to RPA1-aroA mutant at 4X virus, we compared H3.3 deposition at these two concentrations and found that RPA1-aroA mutant was defective in H3.3 deposition compared to wild type RPA1. The expression of RPA1-CM mutant was low compared to wild type, and its effect on H3.3 deposition was not used for comparison. (F-G) Overexpression of RNase H1 impairs deposition of newly synthesized H3.3 at promoters and enhancers**.** Overexpression of RNase H1 impairs deposition of newly synthesized H3.3 at 5 out of 7 promoters and enhancers tested. (F) Analysis of deposition of new H3.3 at four selected promoters and three selected enhancers by ChIP-qPCR. The results were from three independent experiments (mean ± SEM, * $p < 0.05$, N=3). (G) Overexpression of RNase H1 and HA-H3.3 was analyzed by Western blot. **Related to Figure 5.**

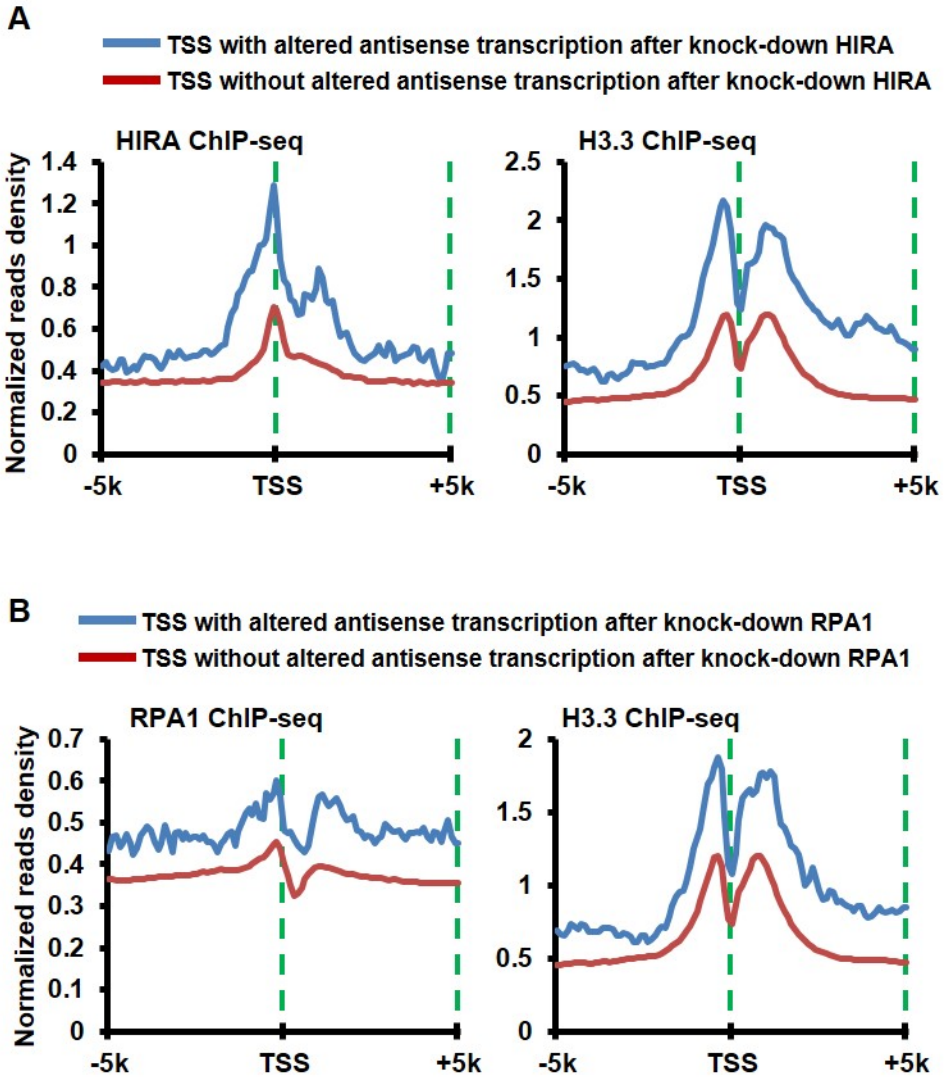
A
TSS with altered antisense transcription after knock-down HIRA
TSS without altered antisense transcription after knock-down HIRA
HIRA ChIP-seq
H3.3 ChIP-seq
Normalized reads density
1.4
1.2
1
0.8
0.6
0.4
0.2
0
2.5
2
1.5
1
0.5
0
-5k
TSS
+5k
B
TSS with altered antisense transcription after knock-down RPA1
TSS without altered antisense transcription after knock-down RPA1
RPA1 ChIP-seq
H3.3 ChIP-seq
Normalized reads density
0.7
0.6
0.5
0.4
0.3
0.2
0.1
0
2
1.5
1
0.5
0
-5k
TSS
+5k

Figure S6. (A-B) HIRA, RPA1 and H3.3 are enriched at TSS regions with altered nascent divergent transcription compared to those without alterations after HIRA depletion (A) or RPA1 depletion (B). (A) Normalized read density plots based on HIRA and H3.3 ChIP-seq experiments at TSS±5 Kb. (B) Normalized read density plots based on RPA1 and H3.3 ChIP-seq at TSS±5 Kb. The TSSs were grouped into two groups based on whether divergent transcription was significantly altered after HIRA knockdown (A) or RPA1 depletion (B). **Related to Figure 6.**

Table S1. A list of genes and shRNAs used for the shRNA screen. Related to Figure 1

Table S2. The original results from each step of screening. First screen lists 81 candidate genes from the first step of screen 246 candidate genes. Second screen lists 21 candidates from the second round of screen of 81 genes. Third screen lists 14 candidates

from analyzing 21 candidates using individual shRNAs. Four screen list the 5 candidates that when deleted affect H3.3 deposition using both IF and chromatin fractionation assays. Related to Figure 1

Table S3. Information for shRNAs Related to Figure 1

shRNA	TRC_ID	Target Sequence
shCHD2-1	TRCN0000021334	CCCTCAAATGAGCCCGAATAT
shCHD2-2	TRCN0000021335	GCCTCTAAGAAGGAACGGATA
shG9a-4	TRCN0000416235	AGATTGAGCCTCCGCTGATTT
shG9a-5	TRCN0000437848	GGACCTTCATCTGCGAGTATG
shING2-1	TRCN0000019217	CTGGACAACAAATATCAAGAA
shING2-2	TRCN0000019218	CATGTGTTTCACTTACCTATA
shUSP51-1	TRCN0000038852	CGTGCTACATAGACACAGCAA
shUSP51-2	TRCN0000038849	GCCTGCAATCAGATGTCACAT
shRPA3-1	TRCN0000018860	GCTAGCTCAATTCATCGACAA
shRPA3-2	TRCN0000018864	CCACCATCTTGTGTACATCTT
shRPA1-1	TRCN0000318750	CCCTAGAACTGGTTGACGAAA
shRPA1-4	TRCN0000318753	GCGGCTACAAAGCGTTTCTTT
shRPA2-1	TRCN0000231920	ACATTGTGCCCTGTACTATAT
shRPA2-3	TRCN0000231922	ATATTCTGGAAGTGATCAATG
shHIRA	TRCN0000232156	CTCTATCCTCCGGAATCATTC

Table S4. Primer Sequences Used for RT-PCR. Related to Figure 1

RT-PCR	Forward primer	Reverse Primer
RPA3	5' AGCTCAATTCATCGACAAGCC 3'	5' TCTTCATCAAGGGGTTCCATCA 3'

Table S5. Primer Sequences Used for CHIP Assay Related to Figure 4 and Figure 5

CHIP-PCR	Forward primer	Reverse Primer
TSS1-2K	5' GGTTGCAGGGCTTGTTGATG 3'	5' TCCCATCATGTCACTGCCTG 3'
TSS1	5' GAGGGGCAGAGGAAATTCGG 3'	5' TACTTTCCCAGACTCCGTGC 3'
TSS1+2K	5' GGAACCCAGCAGAAACCCTT 3'	5' TCACCCTTCCTTAGCCTTGC 3'
TSS2-2K	5' GAGAAGCCATACCCATGCCA 3'	5' TGTCCTGGCTGGCTCATTTT 3'
TSS2	5' GGAGAGGACAGTGATGTCGG 3'	5' TCTAGTCCGCTCTCCTTCCG 3'
TSS2+2K	5' TGGTGGAGGCAAGCAACTTA 3'	5' AGCAGTCTGGTACAGTGGGA 3'
TSS3-2K	5' GCCCACTAGTTTTTGCAGGC 3'	5' TCAGACGTATGTTTGAGGTAGCC 3'
TSS3	5' GAGGCATAGGCGGTTCCC 3'	5' AGCTCACGTTTCTACCCGAG 3'
TSS3+2K	5' ATGGGGAGGCCATTGAACAG 3'	5' TGCCTTCCTCTACTCTCCCC 3'
TSS4	5' GGAGAGGACCCCTAGGAATTG 3'	5' CAGATTGTGTGCATTTTACTGTGT 3'
TSS5	5' CCCCCAGACTCAGACTCTCC 3'	5' CGCTGGGCTCGTTGCTG 3'
Enhancer1	5' GCATGGTAGTCTCCCACTGATTT 3'	5' CTGCAAATTCCTGCTGACTCAC 3'
Enhancer2	5' AGAGGGTGATGGGACGAGAA 3'	5' CCAAGGCTCATGCAGGGAAT 3'
Enhancer3	5' GCAGAGACTTCCCCCTTCTG 3'	5' GCCTTCTCAGAAACCAGGAGA 3'

SUPPLEMENTAL EXPERIMENTAL PROCEDURES

Cell culture, Transfection and Infection

HeLa and 293T cells were grown in Dulbecco's Modified Eagle's medium (Gibco) supplemented with 10% FBS and 1% penicillin/streptomycin. A03_1 cell line carrying an

array of LacO operators was cultured in F-12 Ham's medium (Gibco) supplemented with 10% FBS and 1% penicillin/streptomycin (Invitrogen). HeLa cells stably expressing H3.3-SNAP were grown in the presence of 250 μg/mL G418. 293 cell lines stably expressing H3.1-Flag or H3.3-Flag were grown in the presence of 0.5 μg/mL puromycin. Transient transfection was performed with Lipofectamine 2000 (Invitrogen) according to the manufacturer's instructions. Lenti-virus for shRNA delivery was produced using 293T cells.

ShRNAs, Plasmids and Antibodies

All plasmids for shRNA in pLK0.1 vector were purchased from Sigma (see supplemental Table S1 and S3). PdT11 (for expressing RPA complex in *E. coli*) and RPA1-, 2-, 3-EGFP were provided by Dr. Marc S. Wold. RPA-AB-His, RPA-CDE core-His and RPA-DE-His were gifted by Dr. Gloria E. O. Borgstahl. RPA1-, RPA2- and RPA3-mCherry-LacI were subcloned from PdT11 into mCherry-LacI vector (provided by Dr. Guohong Li). The plasmid of Tsin-RPA1-nuc-myc resistant to shRPA1-1 is subcloned from RPA1-EGFP into pENTR4-nuc-myc, and generated site-directed mutagenesis for resistance to shRPA1-1, then cloned to Tsin-PGKpuro2. H3.3-SNAP was constructed by cloning H3.3 cDNA into pSNAP vector (New England Biolabs). Histones H3.3 or H3.1 cDNA was cloned into pEGFP-C1 vector or mCherry-LacI vector for LacI-LacO targeting, into pQCXIP vector for co-immunoprecipitation and chromatin immunoprecipitation studies. HIRA or UBN1 was cloned into EGFP-N1 vector for LacI-LacO targeting and co-immunoprecipitation studies, into mCherry-LacI vector for co-immunoprecipitation studies, or into pGEX-5X1 for expression in *E. coli*. All site-directed mutagenesis experiments were carried out with

Phusion polymerase (New England Biolabs) and mutations were confirmed by Sanger sequencing. Antibodies against RPA1 and RPA2 were purchased from CalBiochem or gifted by Dr. Bruce Stillman. Anti-HIRA were purchased from Millpore or gifted by Dr. Peter D. Adams. Anti-GFP, UBN1 and p60 were purchased from Abcam. Anti-Tubulin and Flag were purchased from Sigma. Anti-DAXX was purchased from Millipore. Anti-HA was from hybridoma cell line (clone 12CA5). Anti-γH2Ax (Millipore, clone JBW301).

Identification of genes involved in H3.3 deposition through shRNA screens

HeLa cells stably expressing H3.3-SNAP were infected with viruses expressing shRNAs targeting each of 246 genes. Pre-existing H3.3-SNAP proteins were quenched with a blocking reagent 72 h after infection. Cells were reacted with TMR to label newly synthesized H3.3-SNAP in living cells 12 hours after removal of the blocking reagent. The cells were first pre-extracted and then fixed for detection of newly synthesized H3.3-SNAP on chromatin using fluorescence microscopy. In addition, chromatin fractionation assays (CFA) were performed to detect newly synthesized H3.3-SNAP on chromatin. Candidate genes were identified through multiple steps. First, newly synthesized H3.3-SNAP on chromatin was detected using fluorescence microscopy in the cells infected with virus-expressing pooled shRNAs targeting each gene in the library. The candidate genes (81) were analyzed using pooled shRNA. At the same time, the expression levels of total H3.3-SNAP and HIRA, as well as the levels of nascent transcripts detected by 5-ethynyl uridine (EU) staining were analyzed. After exclusion of shRNAs that dramatically affected the expression of HIRA, total H3.3-SNAP or signal of EU staining, 21 candidate genes were

identified and analyzed further using individual shRNAs. 14 candidate genes that when depleted with at least two individual shRNA showed defects in newly synthesized H3.3 deposition were chosen for further analysis using chromatin fractionation assays.

Protein Expression and Purification

We followed standard procedures to express recombinant proteins in *E.coli*. RPA complex were purified as described previously using a series of chromatography including Affi-gel Blue, Hydroxyapatite, and Mono Q columns (Henricksen et al., 1994; Prakash et al., 2011). RPA-AB, RPA-CDE-core, and RPA-DE with His-tags were transformed into Arctic express RIL competent cells. Proteins were induced using 0.3 mM IPTG at 12 ºC overnight. The fusion proteins were purified using Nickel column chromatography and elute with 250 mM imidazole. GST-HIRA-A proteins were induced using 0.15 mM IPTG at 18 ºC overnight, and fusion proteins were purified using GST beads and eluted with 50 mM glutathione.

RPA1, RPA2, HIRA and H3.3-HA chromatin immunoprecipitation (ChIP) assays

To perform RPA1, RPA2 and HIRA ChIP, HeLa cells were crosslinked with 2mM DSG (disuccinimidyl glutarate, Sigma-Aldrich) in PBS for 30 min at room temperature, followed by treatment with 1% formaldehyde for 15 min. After quenching with 125 mM glycine, the cells were harvested and digested by MNase (NEB, M0247S，0.5 U/1000 cells) at 37°C for 20 min to produce soluble chromatin with DNA fragments in the range of

150–300 bp. The lysates were then sonicated for 5 min (30 sec on / 30 sec off) using Bioruptor Twin (UCD-400) (Diagenode, Inc., Denville, NJ) and centrifuged at 21,130 x g for 10 min. The supernatants were collected and the chromatin content was immunoprecipitated using antibodies against RPA1, RPA2 or HIRA overnight. After addition of protein G beads for 3 h, bound chromatin was washed extensively, was eluted and reverse-crosslinked at 65°C overnight using elution buffer. ChIP DNA was purified using Mini-Elute PCR purification kit after the treatment of RNase A and proteinase K and ChIP DNA was analyzed using primers indicated in Table S3 and real time PCR and normalized against input DNA.

LacO and LacI Targeting Assays in A03_1 Cell Line

A03_1 cell line carrying the array of LacO operators were seeded onto glass coverslips for about 24 h. Plasmids (EGFP tag and mCherry-LacI tag) were co-transfected into the cells using X-tremeGENE DNA transfection reagent (Roche) according to the manufacturer's instructions. Cells were pre-extracted with 0.5% Triton X-100 extraction buffer 24 h after transfection and fixed in 3% paraformaldehyde for 15 min, washed with PBS and stained with DAPI for 10 min. Images were captured using a fluorescence microscope equipped with a 100× oil-immersion lens.

Immunoprecipitation and GST Pull-down

To immunoprecipitate H3.1-Flag or H3.3-Flag, 293T cell lines stably expressing H3.1-Flag or H3.3-Flag were lysed using the buffer (50 mM HEPES–KOH, pH 7.4, 200 mM NaCl, 0.5% NP40, 10% glycerol, 1 mM EDTA and proteinase inhibitors) and homogenized for 30 times by dounce homogenizer. After clarification by centrifugation, 7.5 μl ethidium-bromide (10 mg/ml) was added to the lysates. After incubation for 30 min at 4°C, the lysates were cleared by centrifugation and incubated with 20 μl anti-Flag M2 beads at 4°C for 4 h. The beads were washed using washing buffer (50 mM HEPES–KOH, pH 7.4, 100 mM NaCl, 0.01% NP40, 10% glycerol, 1mM EDTA and proteinase inhibitors) five times for 5 min. Proteins bound to beads were eluted with 2 mg/mL Flag peptides. The eluted proteins were precipitated using TCA, dissolved with 1×SDS sample buffer, and analyzed by Western blot.

To immunoprecipitate EGFP tagged proteins, 293T cells were transfected with EGFP expression vectors and lysates were prepared by as described above. EGFP fusion proteins were immunoprecipitated using GFP antibodies. Immunoprecipitated proteins were dissolved in 1×SDS sample buffer and analyzed by Western blot.

To perform GST pull-down assay, 4 μg of GST or GST-fused HIRA-A mutant proteins were immobilized on 20 μl of Glutathione Sepharose 4 Fast Flow (GE Healthcare) resin for 1h at 4°C. The beads were washed once with binding buffer (25 mM Tris-HCl, pH 7.5, 200 mM NaCl, 0.01% NP-40, with protein inhibitors), and then mixed with 4 μg purified RPA complex or other RPA mutant proteins in 0.5 ml binding buffer in the presence of 80 μg/ml ethidium bromide and 100 μl S1 nuclease (Promega) and rotated overnight at 4°C. The

beads were then washed three times with 1 ml of binding buffer containing 300 mM NaCl. Bound proteins were eluted using SDS sample buffer, resolved on a SDS-PAGE gel and detected by Western blot. For GST pull-down assay with MNase treatment(Micrococcal Nuclease), we followed protocol as described by Nguyen(Nguyen and Goodrich, 2006).

RNA-seq and Quantitative RT-PCR

Total RNA was extracted using the miRNeasy Mini Kit (Qiagen #217004) for RNA-seq library preparation or RT-PCR. RNA-seq libraries were prepared with Ovation RNA-seq system v2 kit (NuGEN) according to the manufacturer's instruction, and were sequenced on an Illumina HiSeq 2000 at the Mayo Clinic Center for Individualized Medicine Medical Genomics Facility. For RT-PCR, cDNA was synthesized from 1 μg of total RNA using random hexamer (Invitrogen). Real-time PCR was performed in a 25μL reaction containing 0.1 μM gene-specific primers and SYBR Green PCR Master Mix (Bio-Rad).

Chromatin Immunoprecipitation-deep Sequencing (ChIP-seq)

For RPA1, RPA2 ChIP-seq, we followed single-strand DNA library preparation protocol as previously to prepare library (Meyer et al., 2012; Yu et al., 2014). Analysis of RPA1 and RPA2 ChIP-seq using strand-specific analysis did not reveal whether RPA1 and RPA2 bound to double stranded or single-stranded DNA. HIRA ChIP-seq libraries were prepared from 10 ng ChIP and input DNA using the Ovation ultralow DR Multiplex kit (NuGEN, San Carlos, CA). The ChIP-seq libraries were sequenced to 51 base pairs from both ends on an Illumina HiSeq 2000 at the Mayo Clinic Center for Individualized Medicine Medical

Genomics Facility.

ChIP-seq Data Analysis

Paired-end reads from ChIP-seq were aligned to the human genome (hg19) using the Bowtie2 (Langmead and Salzberg, 2012) software with default parameters. After removal of PCR duplicate by samtools (Li et al., 2009), consistent pair reads were used next-step analysis. Genome-wide read coverage was calculated by BEDTools (Quinlan and Hall, 2010) and in-house Perl programs, and visualized using Integrative Genomics Viewer (Thorvaldsdottir et al., 2013). The reads density scan was performed by in-house Perl programs using the traditional normalization method: Reads Per Kilobase per Million Mapped Reads (RPKM). The ChIP-seq peaks were identified using MACS2 (Zhang et al., 2008) using 0.001 as the cutoff p value.

Clustering RPA ChIP-seq Peaks

RPA1 and RPA2 overlapping ChIP-seq peaks were used in cluster analysis. Peaks were compared against promoter (2 Kb upstream and 1 kb downstream of TSS), HIRA, UBN1, ASF1a, and H3.3 peaks from the previously published work (Pchelintsev et al., 2013), transcription factor ChIP-seq in HeLa cell lines (BRCA1, C-FOS, C-JUN, C-MYC, CHD2, INI1, SMC3, RFX5, POL2, MXL1, P300, H2A.z, HCFC1), regions enriched with histone modifications (H3K4me1, H3K4me2, H3K4me3, H3K27me3, H3K9me3, H3K27ac), and DNase I hypersensitive sites (DnaseHS) obtained from the ENCODE project. RPAs peaks were scored as overlapping if intersected with one or more regulation elements by at least 1bp. The matrix data of RPA overlapping with the regulation elements were clustered by

Cluster software (http://bonsai.hgc.jp/zmdehoon/software/cluster/software.htm#ctv). Clustering results were visualized with the TreeView program (Saldanha, 2004).

Bru-seq Data Analysis

Sequence reads from Bru-seq were aligned to the human genome hg19 with a guide known genes annotations from Refseq using TopHat v2.05 (Trapnell et al., 2009). After removing PCR duplication by samtools (Li et al., 2009), the unique mapping reads were used for analysis. Genome-wide read coverage was calculated by RSeQC (Wang et al., 2012) and in-house Perl programs. The coverage of Watson and Crick strands was calculated separately and visualized using Integrative Genomics Viewer (Thorvaldsdottir et al., 2013). In order to compare nascent RNA levels between NT and samples for HIRA depletion or RPA1 depletion, sense and divergent reads within TSS±2 Kb were counted. Only TSSs separated by least 2 Kb were analyzed. DESeq (Love et al., 2014) was used to calculate the P value. Significantly changed transcripts were identified using a cutoff p value less than 10^{-5}.

Supplemental References

Henricksen, L.A., Umbricht, C.B., and Wold, M.S. (1994). Recombinant replication protein A: expression, complex formation, and functional characterization. The Journal of biological chemistry *269*, 11121-11132.

Hnisz, D., Abraham, B.J., Lee, T.I., Lau, A., Saint-Andre, V., Sigova, A.A., Hoke, H.A., and Young, R.A. (2013). Super-enhancers in the control of cell identity and disease. Cell *155*, 934-947.

Langmead, B., and Salzberg, S.L. (2012). Fast gapped-read alignment with Bowtie 2. Nat Methods *9*, 357-359.

Li, H., Handsaker, B., Wysoker, A., Fennell, T., Ruan, J., Homer, N., Marth, G., Abecasis, G., and Durbin, R. (2009). The Sequence Alignment/Map format and SAMtools. Bioinformatics *25*, 2078-2079.

Love, M.I., Huber, W., and Anders, S. (2014). Moderated estimation of fold change and dispersion for RNA-seq data with DESeq2. Genome Biol *15*, 550.
Meyer, M., Kircher, M., Gansauge, M.T., Li, H., Racimo, F., Mallick, S., Schraiber, J.G., Jay, F., Prufer, K., de Filippo, C.*, et al.* (2012). A high-coverage genome sequence from an archaic Denisovan individual. Science *338*, 222-226.
Nguyen, T.N., and Goodrich, J.A. (2006). Protein-protein interaction assays: eliminating false positive interactions. Nature methods *3*, 135-139.
Pchelintsev, N.A., McBryan, T., Rai, T.S., van Tuyn, J., Ray-Gallet, D., Almouzni, G., and Adams, P.D. (2013). Placing the HIRA histone chaperone complex in the chromatin landscape. Cell Rep *3*, 1012-1019.
Prakash, A., Natarajan, A., Marky, L.A., Ouellette, M.M., and Borgstahl, G.E. (2011). Identification of the DNA-Binding Domains of Human Replication Protein A That Recognize G-Quadruplex DNA. J Nucleic Acids *2011*, 896947.
Quinlan, A.R., and Hall, I.M. (2010). BEDTools: a flexible suite of utilities for comparing genomic features. Bioinformatics *26*, 841-842.
Saldanha, A.J. (2004). Java Treeview--extensible visualization of microarray data. Bioinformatics *20*, 3246-3248.
Thorvaldsdottir, H., Robinson, J.T., and Mesirov, J.P. (2013). Integrative Genomics Viewer (IGV): high-performance genomics data visualization and exploration. Brief Bioinform *14*, 178-192.
Trapnell, C., Pachter, L., and Salzberg, S.L. (2009). TopHat: discovering splice junctions with RNA-Seq. Bioinformatics *25*, 1105-1111.
Wang, L., Wang, S., and Li, W. (2012). RSeQC: quality control of RNA-seq experiments. Bioinformatics *28*, 2184-2185.
Yu, C., Gan, H., Han, J., Zhou, Z.X., Jia, S., Chabes, A., Farrugia, G., Ordog, T., and Zhang, Z. (2014). Strand-specific analysis shows protein binding at replication forks and PCNA unloading from lagging strands when forks stall. Mol Cell *56*, 551-563.
Zhang, M.Q. (2003). Prediction, annotation, and analysis of human promoters. Cold Spring Harbor symposia on quantitative biology *68*, 217-225.
Zhang, Y., Liu, T., Meyer, C.A., Eeckhoute, J., Johnson, D.S., Bernstein, B.E., Nusbaum, C., Myers, R.M., Brown, M., Li, W.*, et al.* (2008). Model-based analysis of ChIP-Seq (MACS). Genome Biol *9*, R137.